Overexpression of Proteins HMGA1 Induces Cell Cycle Deregulation and Apoptosis in Normal Rat Thyroid Cells

Monica Fedele, Giovanna Maria Pierantoni, Maria Teresa Berlingieri, et al.

Cancer Res 2001;61:4583-4590.

[CANCER RESEARCH 61, 4583–4590, June 1, 2001]

Overexpression of Proteins HMGA1 Induces Cell Cycle Deregulation and Apoptosis in Normal Rat Thyroid Cells[1]

Monica Fedele, Giovanna Maria Pierantoni, Maria Teresa Berlingieri, Sabrina Battista, Gustavo Baldassarre, Nikhil Munshi, Monica Dentice, Dimitris Thanos, Massimo Santoro, Giuseppe Viglietto, and Alfredo Fusco[2]

Centro di Endocrinologia ed Oncologia Sperimentale del Consiglio Nazionale delle Ricerche, Dipartimento di Patologia Cellulare e Molecolare, Universita' degli Studi di Napoli "Federico II," 80131 Naples, Italy [M. F., G. M. P., M. T. B., S. B., M. D., M. S.]; Istituto Nazionale dei Tumori, Fondazione Giovanni Pascale, 80131 Naples, Italy [G. B., G. V.]; Department of Biochemistry and Molecular Biophysics, Columbia University, New York, New York 10032 [N. M., D. T.]; and Dipartimento di Medicina Sperimentale e Clinica, Universita' degli Studi di Catanzaro, 88100 Catanzaro, Italy [A. F.]

ABSTRACT

The high mobility group (HMG) proteins (HMGA1a, HMGA1b, and HMGA2) bind to DNA and interact with various transcriptional factors. Therefore, they play an important role in chromatin organization. HMGA protein expression is low in normal adult tissues, but abundant during embryonic development and in several experimental and human tumors. Blockage of HMGA expression inhibits the transformation of rat thyroid PC Cl 3 cells treated with oncogene-carrying retroviruses, thus implicating HMGA in rat thyroid transformation. To better understand the role of HMGA and to establish whether its up-regulated expression is sufficient to induce the transformed phenotype, we generated PC Cl 3 cells that overexpress the protein. We demonstrate that HMGA1b protein overexpression does not transform normal rat thyroid PC Cl 3 cells, but it deregulates their cell cycle: cells enter S-phase earlier and the G_2-M transition is delayed. HMGA1-overexpressing cells undergo apoptosis through a pathway involving caspase-3 activation, probably consequent to the conflict between mitogenic pressure and the inability to proceed through the cell cycle. Using various *HMGA1b* gene mutations, we found that the third AT-hook domain and the acetylation site K60 are the protein regions required for induction of apoptosis in PC Cl 3 cells. In conclusion, although HMGA1 protein overexpression is associated with the malignant phenotype of rat and human thyroid cells, it does not transform normal thyroid cells in culture but leads them to programmed cell death.

INTRODUCTION

The HMG[3] proteins HMGA1a and HMGA1b are nonhistone nuclear proteins encoded by the same gene, *i.e.*, *HMGA1*, through alternative splicing (1). They belong to the HMGA protein family, which includes HMGA2, a protein closely related to HMGA1, but which is encoded by another gene (2). The NH_2 terminus of all HMGA proteins carries three basic DNA-binding domains that bind AT-rich sequences in the minor groove of DNA, and a highly acidic COOH-terminal domain of 15 aa (3). Although not exerting transcriptional activity, HMGA proteins are considered architectural transcription factors because they are involved in organizing chromatin into the architecture required for the basal transcription machinery (4–9).

Disruption of the *HMGA2* gene results in a mouse pygmy phenotype and a decreased growth rate of embryonic fibroblasts (10), which suggests that protein HMGA2 plays a role in cell proliferation. Indeed, HMGA proteins have been immunolocalized *in vivo* to the AT-rich G/Q and C bands of mammalian metaphase chromosomes. Therefore, they could be involved in the changes in chromosome structure that occur during the cell cycle. In addition, HMGA proteins are efficient substrates for cdc2 kinase phosphorylation that alters HMGA DNA-binding affinity in a cell cycle-dependent fashion (11–13).

HMGA protein concentrations are high during embryogenesis (10, 14) and low in normal adult tissues. Increased expression of HMGA proteins is associated with the transformation of rat thyroid cells (15–17), and *HMGA* genes play a pivotal role in thyroid cell transformation (18). In fact, thyroid cells infected by oncogenic retroviruses failed to exhibit phenotypic markers of neoplastic transformation when HMGA protein synthesis was specifically inhibited by antisense constructs. *HMGA1* gene overexpression is a constant feature of human malignant neoplasias (19–21), and blockage of *HMGA1* expression in human thyroid anaplastic carcinoma cell lines results in apoptotic cell death (22).

Rearrangements of the *HMGA2* gene are frequent in human benign tumors of mesenchymal origin. They consist in the loss of the COOH-terminal tail and the fusion with ectopic sequences. Alterations of the *HMGA1* gene also occur in several benign tumors, but they often result in gene overexpression rather than truncation (23–26). In fact, we recently described a case of thyroid microfollicular adenoma with an extragenic translocation in the *HMGA1* locus that caused overexpression of the gene (27).

Because HMGA proteins are necessary for the induction of the transformed phenotype in rat thyroid cells (18), we investigated whether overexpression of the HMGA1b protein is sufficient to induce cellular transformation. To this purpose, we transfected the PC Cl 3 cell line (28), a normal rat thyroid cell line expressing all of the typical markers of thyroid differentiation, with the HMGA1b cDNA under the transcriptional control of the cytomegalovirus promoter. Although the transfected cells entered the S phase earlier than normal cells, they stopped replicating at G_2-M phase and underwent programmed cell death. The third AT-hook domain and the acetylation site K60 are required for HMGA1b-induced apoptosis. The HMGA1a isoform exerts similar biological effects. Taken together, these data demonstrate that HMGA1b alone does not transform normal rat thyroid cells and implicate HMGA1 proteins in the regulation of cell cycle and apoptosis.

MATERIALS AND METHODS

Plasmids. To construct the HMGA1b expression plasmid the full-length HMGA1b cDNA was subcloned into the *Hin*dIII site of the expression vector pRc/CMV (Invitrogen) containing the gene for resistance to G418. HA-tagged HMGA1b expression plasmids containing the entire and various separate portions of the HMGA1b coding sequence were obtained by PCR amplification and subcloned into the pCEFL-HA expression vector (gift of Dr. Sievio Gutkind, NIH, Bethesda, MD): pHA-Y (aa 1–96) contains the entire coding sequence; pHA-Y/T (aa 1–79) contains the first 79 aa, including the three AT-hook domains; pHA-Y1–63 (aa 1–63) contains the first 63 aa, including

Received 7/10/00; accepted 3/26/01.

The costs of publication of this article were defrayed in part by the payment of page charges. This article must therefore be hereby marked *advertisement* in accordance with 18 U.S.C. Section 1734 solely to indicate this fact.

[1] Supported by the Associazione Italiana Ricerca sul Cancro, Consiglio Nazionale delle Ricerche, Ministero dell'Università e Ricerca Scientifica e Tecnologica, and fellowships from Federazione Italiana Ricerca Cancro (to G. M. P. and G. B.).

[2] To whom requests for reprints should be addressed, at Dipartimento di Biologia e Patologia Cellulare e Molecolare, Universita' degli Studi di Napoli "Federico II," via Pansini 5, Italy. Phone: 39-081-7463056; Fax: 39-081-7463037 or 39-081-7701016; E-mail: afusco@napoli.com or alfusco@unina.it.

[3] The abbreviations used are: HMG, high mobility group; HA, hemagglutinin; aa, amino acid; 6H, six hormones; z-VAD-fmk, carbozenzoxy-Val-Ala-Asp-fluoromethyl ketone; Ac-YVAD-cho, carbobenzoxy-Tyr-Val-Ala-Asp-7-amino-4-trifluoromethylcoumarin; z-DEVD-cho, carbobenzoxy-Asp-Glu-Val-Asp-fluoromethyl ketone; z-FA-cho, carbobenzoxy-Phe-Ala-fluoromethyl ketone; CDK, cyclin-dependent kinase; PARP, poly-(ADP-ribose) polymerase; TUNEL, terminal deoxynucleotidyl transferase-mediated nick end labeling.

the first two AT-hook domains and both the acetylation sites; pHA-Y1–53 (aa 1–53) contains the first 53 aa, including the first two AT-hooks and lacks both the acetylation sites K54 and K60; pHA-YmutA contains the entire coding sequence (aa 1–96) with a substitution of aa 53–60, which includes acetylation sites K54 and K60, with the AAIESDPE sequence (29); pHA-YK54 contains the entire coding sequence (aa 1–96) with a mutation on the first acetylation site (K54→A); pHA-YK60 contains the entire coding sequence (1–96) with a mutation on the second acetylation domain (K60→E); pHA-YK54,K60 contains the entire coding sequence (aa 1–96) with mutations on both acetylation sites (K54→A, K60→E). pHA-I (aa 1–107) contains the entire coding sequence of the HMGA1a isoform.

Cell Culture and Transfection Experiments. PC Cl 3 cells are described elsewhere (28). They were grown in Ham's F-12 medium, Coon's modification (Sigma Chemical Co.) supplemented with 5% calf serum (Life Technologies, Inc., Paisley, PA) in the presence of a mix containing six growth factors (6H: 10 nM thyrotropic hormone, 10 nM hydrocortisone, 100 nM insulin, 5 μg/ml transferrin, 5 nM somatostatin, and 20 μg/ml glycyl-histidyl-lysine). The calcium phosphate procedure was used for transfections (30). PC Cl 3 cells were transfected with the above-described plasmids or with the backbone vector. Stable transfectants PC/Y were selected for neomycin resistance in 400 μg/ml G418.

RNA Isolation and Northern Blot Analysis. Total RNA was extracted from the G418-selected cell clones with the RNAfast Isolation System (Molecular System, San Diego, CA). Northern blot hybridization was performed as described previously (31) using Hybond-N membranes (Amersham Pharmacia BioTech Italia) according to the manufacturer's instructions. All cDNA probes were radiolabeled with a random prime synthesis kit (Amersham Pharmacia BioTech Italia). Hybridization reactions were performed at 42°C with 2×10^6 cpm/ml of hybridization solution. After washes, filters were air-dried and exposed to autoradiographic film for 1–7 days. The entire HMGA1b cDNA was used as a molecular probe for the *HMGA1* gene. A mouse glyceraldehyde-3-phosphate dehydrogenase cDNA probe was used to equalize RNA loading.

Protein Extraction, Western Blotting, and Antibodies. Cells were washed once in cold PBS and lysed in a buffer containing 50 mM N-2-hydroxyethylpiperazine-N′-2-ethanesulfonic acid (HEPES; pH 7.5), 1% (v/v) Triton X-100; 50 mM NaCl; 5 mM EGTA, 50 mM NaF; 20 mM Na PP_i; 1 mM sodium vanadate, 2 mM phenylmethylsulfonyl fluoride, and 0.2 mg/ml each of aprotinin and leupeptin. Lysates were clarified by centrifugation at $10{,}000 \times g$ for 15 min, and the supernatant was stored at −70°C. Protein concentration was estimated by a modified Bradford assay (Bio-Rad). Total proteins were separated by SDS-PAGE and transferred to membranes (Immobilon-P Millipore Corp., Bedford, MA). Membranes were blocked with 5% nonfat milk proteins and incubated with the appropriate antibodies. Anti-HMGA1 are polyclonal antibodies raised against a synthetic peptide located in the NH2-terminal region of the HMGA1 proteins (32) at a dilution of 1:1,000; antibodies against various cyclins, CDK, and CDKIs were from Santa Cruz Biotechnology (anti-cyclin D3 C-16, anti-CDK7, C-19, and anti-cyclin B1 GNS1), Oncogene Science (anti-cyclin A AB-2), PharMingen (anti-cyclin E HE12, anti-CDK2, and anti-CDK4), and Calbiochem (anti-cdc2 Ab-1). Anti γ-tubulin (Santa Cruz Biotechnology) was used to equalize the amount of proteins loaded. Bound antibodies were detected by the appropriate secondary antibodies and revealed with the Amersham enhanced chemiluminescence system.

Growth Rate and [^{3}H]thymidine Incorporation. The cells (10^5/dish) were plated in 60-mm plates and cultured in complete medium. They were counted every day for 10 consecutive days to extrapolate the growth curves. The doubling time was measured when the cells were in the logarithmic phase of growth.

To evaluate [^{3}H]thymidine incorporation, the cells were plated as above and allowed to adhere for 12 h in serum-containing medium. They were then washed three times in PBS and left for 3 days in serum-free medium. After 3 days of starvation, the cells were allowed to grow in serum-containing medium and harvested after 0, 12, 24, 48, and 72 h of incubation with pulses of 4 μCi/ml of [^{3}H]thymidine (Amersham Pharmacia BioTech Italia) added to each plate 3 h before each harvesting. The plates were then washed three times with PBS, and the cells were fixed in 5% trichloroacetic acid at 4°C for 20 min, washed three times in trichloroacetic acid and solubilized in 0.5 N NaOH (0.3 ml). This solution was neutralized with 0.5 N HCl (0.3 ml), and radioactivity was measured by liquid scintillation counting. Two plates for each time point were used to analyze growth rate and [^{3}H]thymidine incorporation, and the experiments were performed in triplicate.

Flow-Cytometry. PC Cl 3 and PC/Y cells were analyzed for DNA content as described previously (33). Cells were collected and washed in PBS. DNA was stained with propidium iodide (50 μg/ml) and analyzed with a FACScan flow cytometer (Becton Dickinson, San Jose, CA) that was interfaced with a Hewlett-Packard computer (Palo Alto, CA). Cell cycle data were analyzed with the CELL-FIT program (Becton Dickinson).

Immunoprecipitation Analysis and Kinase Assay. PC and PC/Y cells, starved or treated for 12, 24, and 36 h with complete medium, were lysed in NP40 lysis buffer [50 mM HEPES (pH 7); 250 mM NaCl, 5 mM EDTA, 50 mM NaF, 0.5 mM Na_3VO_4, and 1 mM DTT supplemented with $Na_4P_2O_7$, aprotinin, leupeptin, pepstatin, and benzamidine]. Four hundred μg of extract were incubated with 1 μg of anti-cdc2 Ab-1 (Calbiochem) rabbit polyclonal antiserum or with 1 μg of anti-Cyclin B1 GNS1 (Santa Cruz Biotechnology) mouse monoclonal antibodies for 1 h at 4°C. A/G Sepharose protein (Santa Cruz Biotechnology) was then added, and lysates were incubated for 15 h at 4°C. Immunocomplexes were collected by centrifugation at 10,000 rpm for 1 min at 4°C and washed four times in NP40 lysis buffer. After two additional washes in 10 mM Tris-HCl (pH 6.8), 20 mM $MgCl_2$, one-tenth of the immunoprecipitates was used for kinase assay and nine-tenths were resolved on polyacrylamide gels and probed with anti-cyclin B or anti-cdc-2 antibodies. For *in vitro* kinase assay, immunoprecipitates were resuspended in cdc-2 kinase assay buffer (Upstate Biotechnology) for 20 min in the presence of 2 μg of histone H1 (Upstate Biotechnology) as substrate and 0.5 μCi of [γ-^{32}P] ATP (3,000 Ci/mmol; Amersham Pharmacia Biotech) in a final volume of 25 μl. Samples were incubated for 20 min at 30°C, and the reaction was stopped by adding 25 μl of 2 × Laemmli loading dye. Phosphorylated histone H1 was visualized by autoradiography and quantified with the GS-525 Molecular Imager (Bio-Rad) interfaced with an Hewlett-Packard computer.

Cell Viability, DNA Laddering, and TUNEL Assay. To assess cell viability, nonadherent and adherent cells were collected, and aliquots were mixed with an equal volume of 0.4% trypan blue (Life Technologies, Inc.). The percentage of cells that picked up the dye (dead cells) was determined. The data are representative of at least three independent culture dishes per time point.

For the DNA laddering assay, adherent and nonadherent cells from a 100-mm Petri dish were collected, washed in PBS, and resuspended gently in 0.4 ml of lysis buffer [0.5% Triton X-100, 5 mM Tris-HCl (pH 7.4), 20 mM EDTA]. After a 20-min incubation on ice, the samples were centrifuged at 12,000 rpm for 30 min. The supernatants were extracted with phenol-chloroform and precipitated in ethanol. The pellets were washed in 70% ethanol and resuspended in TE buffer [10 mM Tris (pH 8)-1 mM EDTA] containing 0.4 μg/μl RNaseA. Extracted nucleic acids were treated with RNaseA at 37°C for 30 min and then analyzed on 1.2% agarose gels stained with ethidium bromide.

The TUNEL assay was performed with the *In Situ* Cell Death Detection Kit (Boehringer, Mannheim) following the manufacturer's instructions. Briefly, the air-dried cells were fixed with a freshly prepared paraformaldehyde solution [4% in PBS (pH 7.4)] for 30 min at room temperature. The slides were rinsed with PBS and incubated in permeabilization solution (0.1% Triton X-100 and 0.1% sodium citrate) for 2 min on ice. Then the slides were rinsed twice with PBS, and 50 μl of TUNEL reaction mixture was added. After 30 min incubation at 37°C, substrate solution was added. After 10 min incubation at room temperature the slides were mounted and analyzed under the light microscope.

Inhibition of Cell Death. Cells (4×10^5) were plated in six multiwells and allowed to grow for 4 days before a treatment with 10 and 100 μM of z-VAD-fmk, z-DEVD-cho, Ac-YVAD-cho, and z-FA-cho (Calbiochem) for 72 h. Death was assessed by measuring the percentage of stained cells with trypan blue as described above.

RESULTS

Generation of PC/Y Cells. PC Cl 3 cells were transfected with full-length *HMGA1* cDNA or the backbone vector and selected in a medium containing Geneticin. Several clones and a mass population were isolated for each transfection and analyzed by Northern and Western blot (Fig. 1) for the expression of the transfected gene.

Northern blot analysis showed that PC/Y cells express a specific HMGA1 transcript (Fig. 1*A*). Conversely, no *HMGA1* expression was found in the untransfected (PC Cl 3) or in the backbone vector-transfected PC Cl 3 cells (PC/V; *panel A*). The PC Cl 3 cells transformed with the myeloproliferative sarcoma virus (PC MPSV; 28) expressed the endogenous HMGA1-specific transcript of about 1.8 kb. Western blot analysis with anti-HMGA1 antibody (32) showed an immunoreactive protein in the PC/Y and PC MPSV cells, but not in the parental PC Cl 3 or PC/V cells (Fig. 1*B*). We selected six PC/Y and two PC/V cell clones for additional analyses. All of the clones showed the same biological behavior. Therefore, the data shown here refer to one or two representative clones.

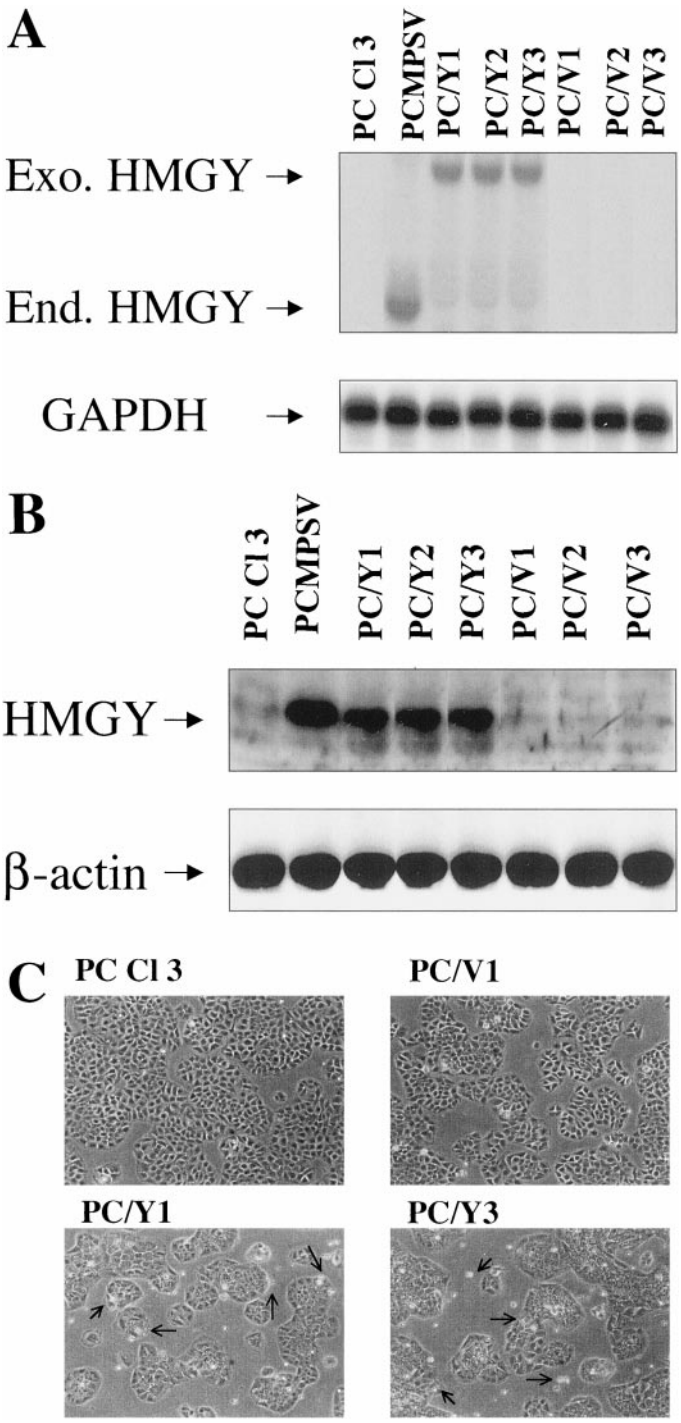

Fig. 1. Isolation of HMGA1b-expressing PC Cl 3 cells and their morphology. *A*, Northern blot of three clones transfected with HMGA1b (PC/Y1–3) or the empty vector (PC/V1–3). A specific transcript corresponding to the transfected *HMGA1* gene appears in all three PC/Y clones. PC/V clones were devoid of HMGA1 expression. Positive control, HMGA1 expression in PC Cl 3 cells infected with the MPSV virus (15). *B*, Western blot of the three clones showed in *A*. *C*, morphology of normal and HMGA1b-transfected PC Cl 3 cells; ×150. *Top*, *left*: PC Cl 3 cells; *top*, *right*: empty vector transfectant (PC/V) clone 1; *bottom*, *left*: HMGA1b transfectant (PC/Y) clone 1; *bottom*, *right*: HMGA1b transfectant clone 3. *Arrows*, apoptotic cells.

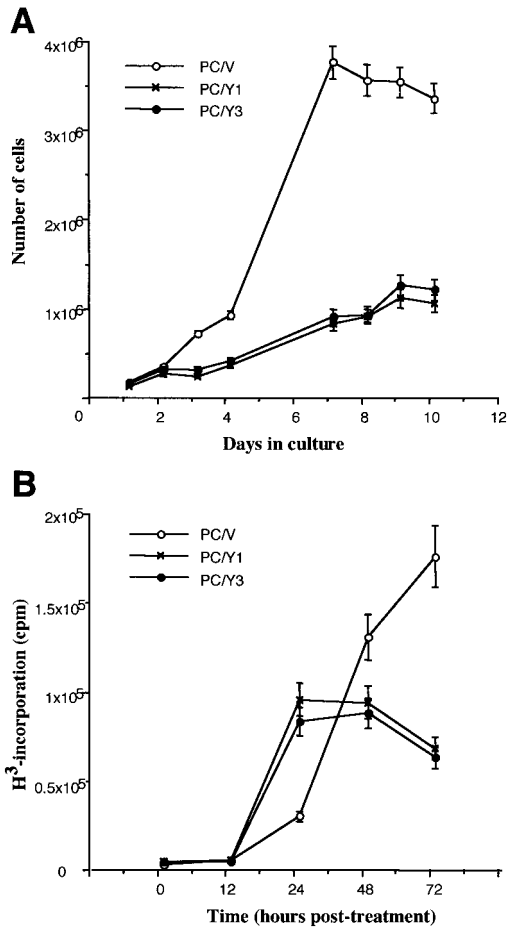

Fig. 2. Growth of HMGA1b-expressing PC Cl 3 cells. *A*, growth curves of PC/V and two representative PC/Y clone cells. Cells were plated as described in "Materials and Methods" and counted daily for 10 days. *B*, [^{3}H]thymidine incorporation in PC/V and two representative PC/Y clone cells. Cells were pulsed with [^{3}H]thymidine as described in "Materials and Methods" and monitored for [^{3}H]thymidine incorporation every 12 h for 72 h. The results are the media of three independent experiments.

The PC/Y cells showed modest morphological changes with several apoptotic bodies and many dead cells floating in the culture medium (Fig. 1*C*). They retained a differentiated phenotype and were not tumorigenic (data not shown).

Growth of PC/Y Cells. The growth potential of the PC/Y cells was evaluated from growth rate and [^{3}H]thymidine incorporation. As shown in Fig. 2*A*, the growth rate of PC/Y cells was reduced compared with PC/V cells. In fact, the doubling time of PC/Y cells (25 ± 3h) was significantly higher than that of PC/V cells (18 ± 3h), suggesting that HMGA1b may inhibit thyroid cell growth. These differences were significant ($P < 0.01$).

To investigate whether the reduced growth rate of PC/Y cells resulted from inhibition of DNA synthesis, [^{3}H]thymidine incorporation was assayed. Cells were synchronized by starvation in serum-free medium for 3 days and subsequently stimulated to reenter the cell cycle by the addition of 6H in the presence of 5% calf serum. Cells were labeled with a 3-h [^{3}H]thymidine pulse and collected every 12 h for 3 days. Surprisingly, PC/Y cells started to incorporate [^{3}H]thymidine at least 12 h before PC/V cells. In fact, after 24 h of treatment,

the percentage of PC/Y cells that incorporated [^{3}H]thymidine was 2.5-fold higher than PC/V cells (Fig. 2*B*). However, the rate of thymidine incorporation of PC/Y cells remained stable, and started to decrease at 48 h. Conversely, the rate of [^{3}H]thymidine incorporation of PC/V cells continued to increase steadily (Fig. 2*B*). These results demonstrate that PC/Y cells enter the cell cycle from serum deprivation-induced G_0 more rapidly than parental PC Cl 3 cells. However, the finding that, at later times, the [^{3}H]thymidine incorporation rate of PC/Y cells is not maintained at levels comparable with those observed in PC/V cells and that the growth rate of PC/Y cells is lower *versus* parental cells, suggests that the constitutive expression of HMGA1b may interfere with the correct completion of the cell cycle, at least in thyroid cells.

Cell Cycle Profile of PC/Y Cells. To verify the results of the [^{3}H]thymidine incorporation assay, the cell cycle distribution of PC Cl 3, PC/V, and PC/Y cells was analyzed. When PC/V cells are starved of serum and hormones for 3 days, they become quiescent (G_0), and can be stimulated to enter the S-phase by 24 h of serum and 6H administration. To determine whether PC/Y cells had a reduced G_1 phase and synthesized DNA earlier than PC/V cells, PC/V and PC/Y cells were starved as described, stimulated to reenter the cycle with serum and 6H, and analyzed by flow cytometry at 0, 12, 24, and 36 h after treatment. The percentage of PC/Y cells in the S-phase compartment increased significantly 12 h after treatment, reaching a peak at 24 h (Fig. 3*B*). Conversely, most PC Cl 3 and PC/V cells were still in G_0/G_1 phase 12 h after treatment (Fig. 3*A*) but entered S-phase 24 h after treatment (Fig. 3*B*). Furthermore, as shown in Fig. 3*C*, the fraction of PC/Y cells in the G_2-M compartment 24 h posttreatment was increased by about 2-fold with respect to PC/V cells (22.9% *versus* 12.3%, respectively). The difference between PC/V and PC/Y cells in the G_2-M compartment was reduced 36 h after treatment. Overall, there were two types of cell cycle profile alterations in PC/Y cells compared with PC/V cells: early entry into S-phase and accumulation of cells in G_2-M phase after 24–36 h of hormone and serum treatment.

Cyclin and CDK Expression in PC/Y Cells. Progression through the cell cycle requires the coordinated activation of a family of protein kinases called CDKs (34). Activation of each kinase is a highly regulated process beginning with: (*a*) the association of a CDK with a positive regulatory subunit called "cyclin"; (*b*) phosphorylation of a conserved threonine residue by a CDK-activating kinase; and/or (*c*) binding of inhibitory molecules, *i.e.*, CDK inhibitors (35–37). G_1 progression is controlled by sequential activation of cyclin D/CDK4–6 and cyclin E/CDK2 complexes, whereas entry into S-phase is mainly regulated by cyclin A/cdk2. Progression of cells through G_2 into mitosis is controlled by sequential activation of cyclin A/Cdk2 and cyclin B/cdc2 complexes.

To investigate the effects exerted by HMG-Y on PC Cl 3 cells, we determined the expression of cyclins, CDK, and CDK-inhibitor proteins in PC/V and PC/Y cells. Cells were starved of 6H and serum as described, stimulated to reenter the cycle after 3 days, and then lysed at 6, 12, 18, 24, and 36 h. Subsequently, the expression of cyclins, CDK and CDK inhibitor proteins was detected by Western blot. Cyclin D3 was the only D-type cyclin detected in PC Cl 3 cells. Cyclin D3 was not expressed in starved PC/V cells, but it was induced after 6 h of stimulation, with a peak at 18–24 h (Fig. 4). Conversely, cyclin D3 expression was elevated in PC/Y cells even when the cells were deprived of growth factors and hormones. Furthermore, cyclin D3 induction in PC/Y cells occurred earlier and peaked at 12 h of treatment. Similarly, the basal level of cyclin E protein was increased in starved PC/Y cells and increased even more after 6 h of treatment, *i.e.*, 12 h earlier than in PC/V cells. This pattern of G_1 cyclin expression coincides with the finding that PC/Y cells enter the cell cycle 12 h earlier than do PC/V cells. CDK2 expression was increased after 18–24 h of treatment in PC/V cells and after 12 h in PC/Y cells. Conversely, CDK4/6 and CDK7 expression was not altered in quiescent or proliferating PC/V or PC/Y cells. These findings coincide with the observation that PC/Y cells failed to arrest growth completely in G_1 upon starvation, and that they enter S-phase 6–12 h earlier than do PC/V cells.

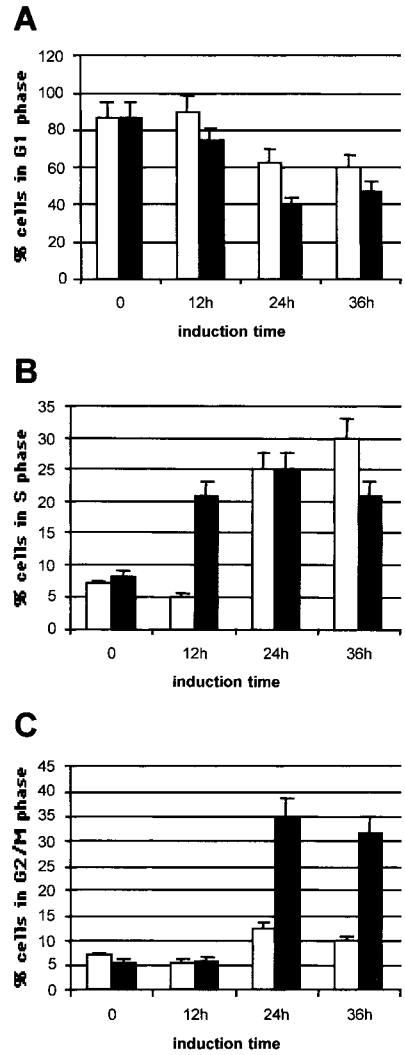

Fig. 3. Flow cytometry of the PC/V and PC/Y cell cycles at various times of serum and hormone stimulation after starvation. Percentages of the cell cycle phase distribution were determined for each cell clone without or with hormones and serum refed for 12, 24, and 36 h. *White* and *black bars*, PC/V and PC/Y cells, respectively.

In PC/V cells cyclin A was increased after 12–18 h of treatment and decreased abruptly at 36 h, whereas in PC/Y cells its expression remained elevated at 36 h. Cyclin B was induced after 18 h in both PC/V and PC/Y cells, but the level of cyclin B was much higher in PC/Y cells compared with PC/V cells, and its expression was still detectable at 36 h in PC/Y cells. Cdc2 expression was induced by serum and hormones in PC/V cells at 18–24 h and was completely down-regulated at 36 h, whereas it was induced at 12 h in PC/Y cells, and its expression was increased at 36 h. Instead, no differences in the expression levels of CDK inhibitors p21, p27, and p57 were detected between PC/V and PC/Y cells (data not shown). These findings are in agreement with the observation that an increased fraction of PC/Y cells are in the G_2-M compartment at 24–36 h of treatment.

cdc2 Activity in PC/Y Cells. A major difference between PC/V and PC/Y cells occurred in the expression of the G_2-M associated

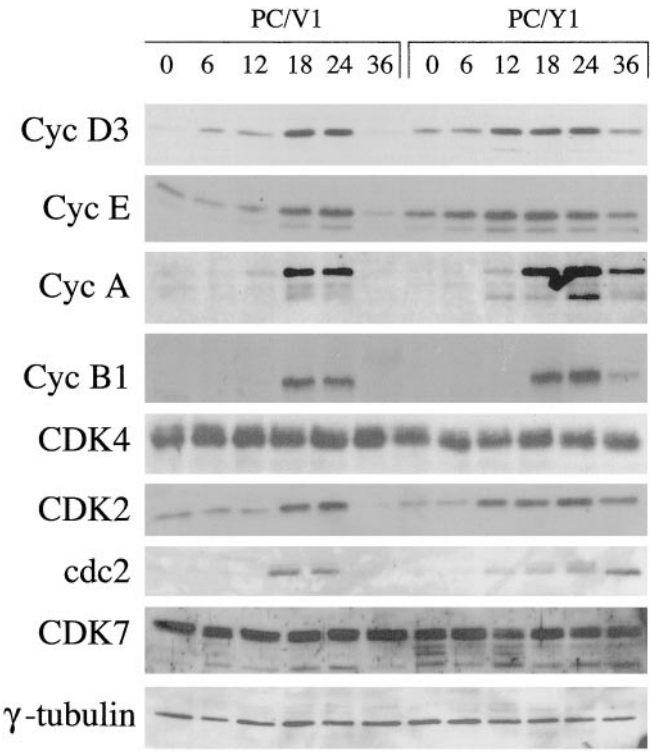

Fig. 4. Expression of cell-cycle regulators in PC/V and PC/Y cells starved (*0*) and stimulated with serum and hormones for 6, 12, 18, 24, and 36 h. The expression of each cell-cycle regulator was determined by Western blot analyses as described in "Materials and Methods."

proteins, cdc-2 and cyclin B. Because activation of cyclin B/cdc-2 complexes regulates G_2-M transition, and its inactivation is a prerequisite for correct completion of the M phase, we compared the activity of cyclin B/cdc-2 complexes in PC/Y cells *versus* PC/V cells. To this aim, PC/V and PC/Y cells were starved for 72 h and then cultured with growth factors and serum for 24 or 36 h. The lysates obtained were analyzed for cyclin B- and cdc-2-associated kinase activity. cdc-2 activity was very low in starved PC/V cells, but was increased 24 h after treatment (Fig. 5, *top*, *Lanes 1–3*). This is consistent with the FACScan result that PC/V cells start to enter G_2-M at 24 h. Differently, the activity of cyclin B/cdc-2 complexes appeared in PC/Y cells at 24 h (like in the PC/V cells), but was increased further at 36 h (Fig. 5, *top*, *Lanes 4–6*). Similar results emerged from the analysis of cyclin B-associated activity (Fig. 5, *bottom*). These data suggest that in PC Cl 3 cells, HMGI-Y protein may interfere with the activity of cyclin B/cdc-2 complexes.

HMGA1b Overexpression Results in Apoptosis of Thyroid Cells. In parallel with the cell cycle analysis, we investigated whether HMGA1b overexpression in PC Cl 3 cells induced cell death. A cell viability analysis (the trypan blue exclusion technique) revealed a striking loss of viable PC/Y cells from 6 days after plating. In contrast, the PC/V cells did not show a significant rate of nonphysiological cell death (Fig. 6*A*). To investigate the mechanisms of PC/Y cell death, we performed three apoptotic assays: DNA laddering, flow-cytometric analysis, and TUNEL assay. As shown in Fig. 6*B*, the PC/Y cells underwent massive DNA fragmentation after 7 days in culture. Conversely, no DNA laddering was observed in PC/V cells.

FACS analyses of PC/V and PC/Y cells at 7 days after plating showed that a consistent fraction (32.1%; 2-fold more than PC Cl 3 and PC/V cells) were in the sub-G_1 compartment (Fig. 5*C*). Similarly, PC/Y but not PC/V cells stained positive at the TUNEL assay (data not shown). These results demonstrate that PC/Y cells undergo apoptosis.

Mechanisms Underlying HMGA1b-induced Apoptosis. Initially, to gain insights into the signaling pathway implicated in HMGA1b-mediated apoptosis, we monitored activation of caspase-3, an interleukin 1β converting enzyme-like cysteine protease that is central to many apoptosis systems (38–41). Total cell extracts were blotted with an antibody raised against PARP, a substrate for active caspase-3 (39, 41), which recognizes the full-length M_r 112,000 PARP and the M_r 85,000 cleaved product observed after apoptotic stimuli (42). The cleavage of PARP in PC/Y cells (Fig. 7*A*) suggests that the caspase-3 pathway is involved in induction of HMGA1b-dependent apoptosis. In contrast, no PARP cleavage was observed in PC/V cells.

We next examined the requirement of caspase activities for HMGA1b-mediated apoptosis by examining the effect of three caspase inhibitors (z-VAD-fmk, Ac-YVAD-cho, and z-DEVD-cho) on PC/Y apoptosis. z-VAD-fmk inhibits almost all caspases examined to date. It blocks or delays cellular apoptosis caused by diverse sets of signals (43) and is not effective on caspase 9 (44). Conversely, Ac-YVAD-cho and z-DEVD-cho are specific inhibitors of the substrates of caspase 1 and caspase 3, respectively. As shown in Fig. 7*B*, z-DEVD-cho prevented HMGA1b-induced apoptosis in a dose-dependent manner, a weak preventive effect was obtained with z-VAD-fmk, and there was no effect with either Ac-YVAD-cho or z-FA-cho. These results indicate that the apoptotic effect associated with the overexpression of the HMGA1b protein in PC Cl 3 cells is caspase-dependent and is mediated by caspase-3.

Subsequently, we analyzed the expression of several genes known to be involved in apoptosis. No differences in *Bcl-2*, *Bax*, *Bcl-X*, and *c-myc* gene expression were observed between PC/V and PC/Y cells (data not shown).

Mapping of the HMGA1b Region Responsible for Induction of Apoptosis. To map the HMGA1b regions required for the induction of apoptotic cell death in PC Cl 3 cells, we used a series of COOH-terminal deletions of the gene (29, 45). These HMGA1b derivatives were transiently transfected on the PC Cl 3 cells, and an apoptotic assay (TUNEL assay) was performed 3 days after. Fig. 8 shows that deletion of the COOH-terminal tail (pHA-Y/T) did not significantly impair HMGA1b-induced apoptosis in PC Cl 3 cells. Conversely, deletion of the last AT-hook domain (pHA-Y1–63) and of the last AT-hook domain plus the region between the middle and the last basic domain (pHA-Y1–53), and also replacement of the region spanning aa

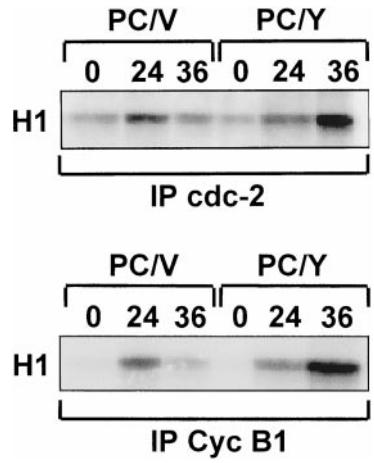

Fig. 5. Cdc-2 and cyclin B1 activity in PC/V and PC/Y cells starved (*0*) and stimulated with serum and hormones for 24 and 36 h. Endogenous cdc-2 (*top*) and cyclin B1 (*bottom*) were immunoprecipitated from cell lysates and assayed by phosphorylation of histone H1 as described in "Materials and Methods."

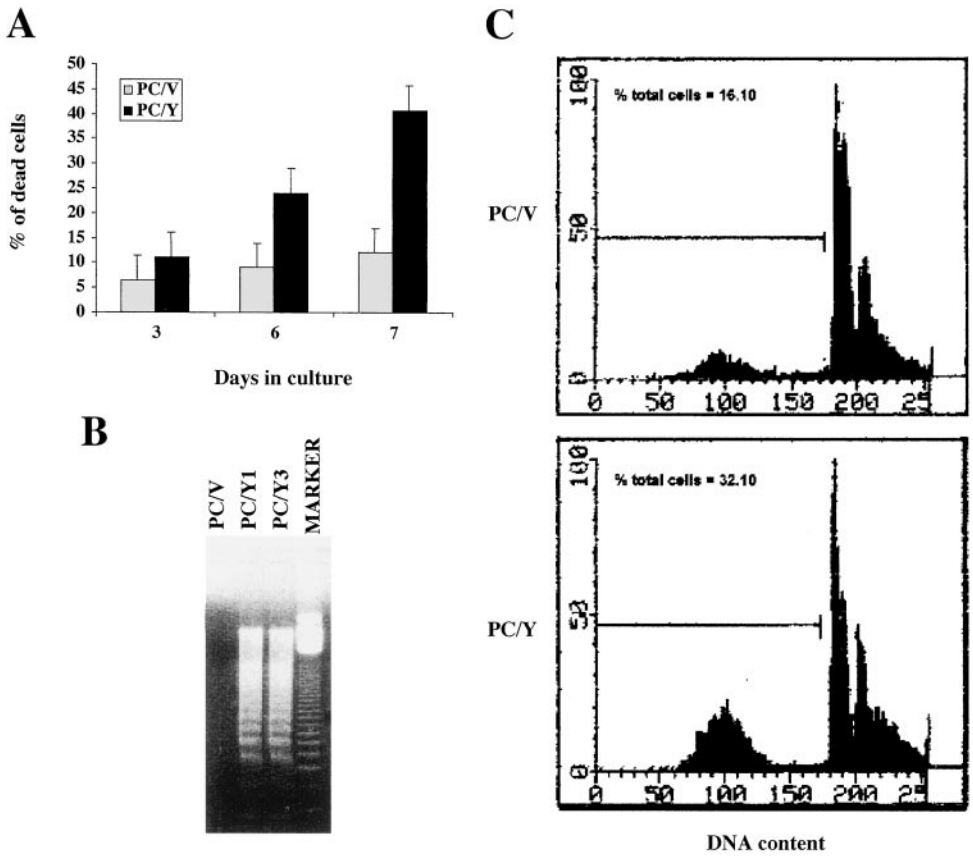

Fig. 6. Cell death and apoptosis. *A*, cell viability measured by trypan blue exclusion assay. The percentage of cell death was calculated as the number of *blue cells*/number of total cells × 100. *B*, DNA fragmentation in PC/V (*Lane 1*) and PC/Y cells (*Lanes 2* and *3*) 7 days after plating. *C*, flow cytometry of PC/V and PC/Y cells. The *horizontal line* delimits the sub-G_1 cell fraction, which is representative of apoptotic cells. The percentage of cells present in this fraction is reported within each frame.

54–63 with an oligonucleotide coding for different aa (pHA-YmutA), drastically reduced the apoptotic effect. This region carries two acetylation sites: lysine 54, which is preferentially acetylated by CBP, and lysine 60, which is preferentially acetylated by P/CAF (29). To determine whether the acetylation sites are important in the apoptotic process, we examined the apoptotic ability of constructs with specific mutations in lysines 54 and 60. The single mutant K54A (pHA-YK54) did not impair apoptosis. Conversely, both the single mutant K60E (pHA-YK60) and the double mutant K54A-K60E (pHA-YK54,K60) inhibited the apoptotic effect. These findings suggest that the third AT-hook domain and/or the P/CAF mediated acetylation of the HMGA1b protein are involved in the induction of apoptosis in PC Cl 3 cells. Finally, we transiently overexpressed in PC Cl 3 the long HMGA1a isoform, which has an extra stretch of 11 aa between the first and second AT-hook domains. As shown in Fig. 8*A*, HMGA1a exerts similar effects on the apoptotic phenotype, suggesting that the mechanisms underlying cell cycle deregulation and apoptosis are the same for both HMGA1 isoforms. A Western blot showing the protein levels of the various transfected genes and mutants is represented in Fig. 8*B*.

DISCUSSION

HMGA1 protein overexpression has been detected in neoplastically transformed cell lines and in human cancer cells originating from a variety of tissues (15–17, 20, 21, 32, 46). This overexpression is directly correlated with the cancer stage (23, 47) and plays a key role in neoplastic transformation (18).

To assess whether the *HMGA1* gene exerts a transforming effect, we transfected the HMGA1b cDNA under the transcriptional control of the cytomegalovirus promoter in normal rat thyroid cells. Surprisingly, HMGA1b overexpression did not induce thyroid cell transformation; instead, it deregulated cell growth and induced apoptosis.

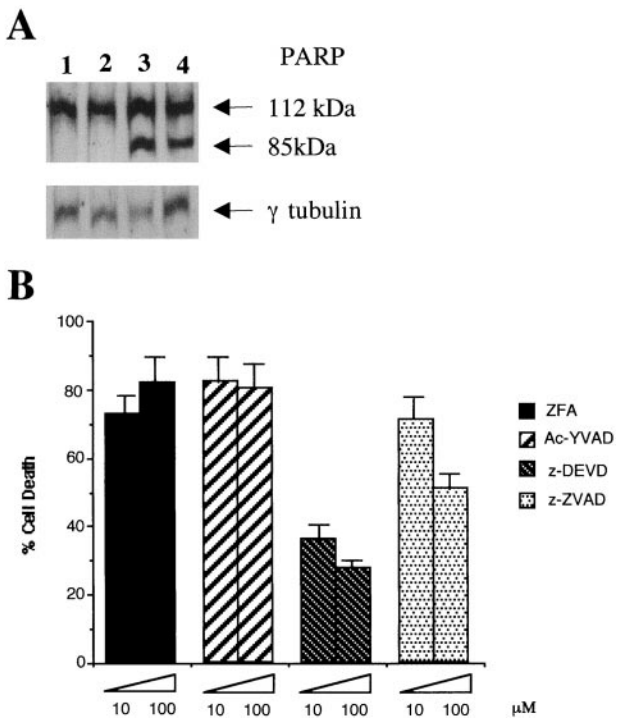

Fig. 7. Apoptotic mechanisms. *A*, specific proteolytic cleavage of PARP by activation of caspase-3 in ectopic HMGA1b-expressing PC Cl 3 cells. Samples (50 μg) of cell lysates were analyzed by Western blot using a specific anti-PARP polyclonal antibody (Santa Cruz Biotechnology). *Lanes 1* and *2*, cell lysates from two PC/V clones; *Lanes 3* and *4*, cell lysates from two PC/Y clones. γ-tubulin expression was also measured to normalize the amount of protein loaded. *B*, effect of four caspase inhibitors on HMGA1b-mediated apoptosis in PC Cl 3 cells. Cells were treated with the specific inhibitor as described in "Materials and Methods." Cell viability, evaluated with trypan blue dyeing, was used to measure the apoptotic effect. z-FA-cho (*ZFA*) served as a negative control.

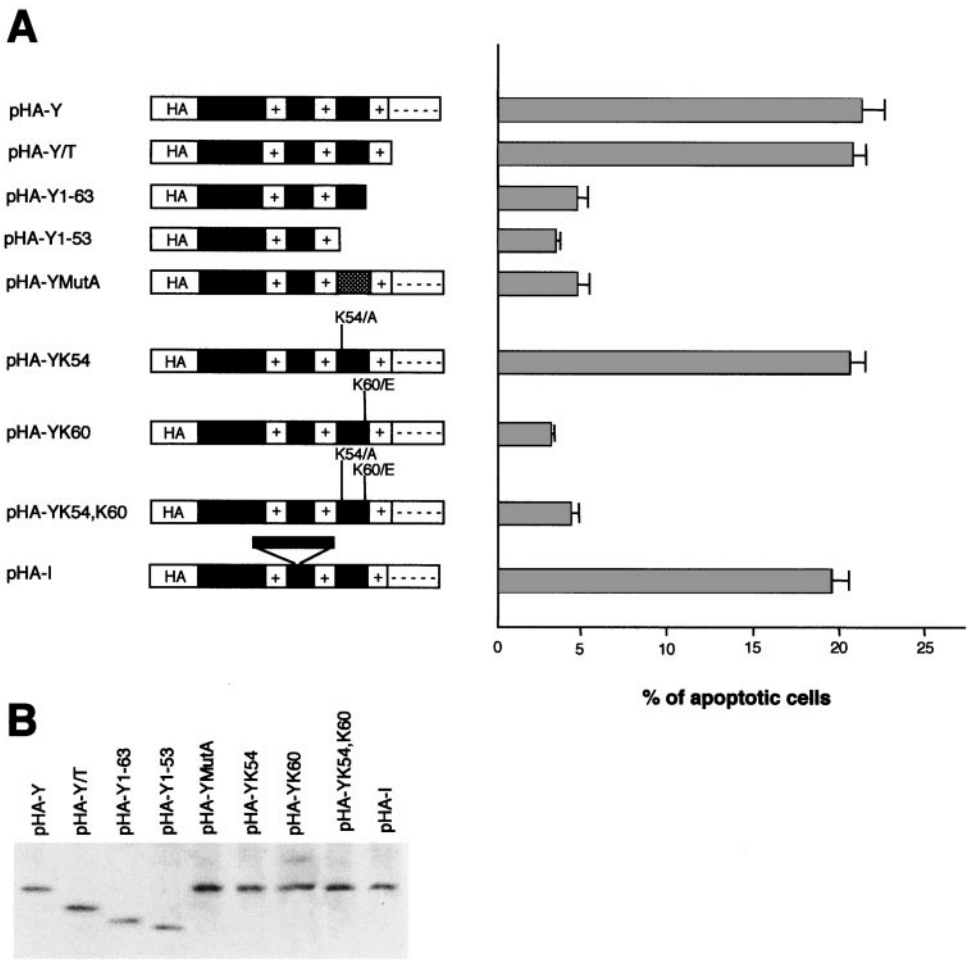

Fig. 8. Mapping of the HMGA1b region involved in apoptosis. *A*, scheme of HMGA1b mutants used in this study and their respective apoptotic potential in PC Cl 3 cells, indicated by the percentage of apoptotic cells measured by TUNEL assay. *B*, Western blot showing protein expression levels of the various mutants.

[^{3}H]thymidine incorporation and flow-cytometric analysis demonstrated that HMGA1b-transfected cells (PC/Y) enter the S-phase compartment significantly earlier than untransfected cells, but they have an abnormally extended G_2-M phase. Expression analysis of cyclins and CDK confirmed these data: the cyclins and CDK involved in the G_1-S transition were expressed earlier, and the expression of the cyclinB1/cdc2 complex involved in exit from G_2-M was more prolonged in PC/Y cells than in vector-transfected cells (PC/V). Moreover, cdc-2- and cyclin B-associated kinase activities peaked 12 h later in PC/Y cells compared with PC/V cells. Because inactivation of cyclin B/cdc-2 is necessary for completion of the M phase, these results suggest that PC/Y cells exit mitosis later than parental PC Cl 3 cells.

Despite the early entry into S-phase, but in agreement with the prolonged G_2-M phase, PC/Y cells grow more slowly than either PC/V or PC Cl3 cells. We found that apoptotic cell death, assessed by three techniques, largely accounts for the reduced cell growth rate of PC/Y cells. In addition, we demonstrate that HMGA1b-induced apoptosis is associated with PARP cleavage and inhibited by the cysteine protease inhibitor z-DEVD-cho in a dose-dependent manner, but not inhibited or partially inhibited by Ac-YVAD-cho and z-VAD-fmk, respectively. The caspase inhibitor z-VAD-fmk does not inhibit caspase 9, whereas it is very effective in inhibiting caspase 3 activity (44). Conversely, the z-YVAD-cho inhibitor is virtually specific in suppressing caspase 1 activity. Consequently, it appears that the caspase 3 rather than the caspase 1 pathway is involved in the programmed cell death caused by *HMGA1b* gene overexpression.

Using deletion mutants, we mapped the regions required for the apoptotic effect in the third DNA-binding domain and in a region spanning from aa 54 to aa 63. The latest region carries two acetylation sites: lysine 54, which is preferentially acetylated by CBP, and lysine 60, which is preferentially acetylated by P/CAF (29). Lysine 60 is involved in the induction of apoptosis because mutation of this lysine impaired HMGA1b-induced apoptosis. In the context of the human β-IFN enhanceosome, acetylation of HMGA1 by CBP, but not by P/CAF, leads to enhanceosome destabilization and disassembly, turning off *IFNβ* gene expression (29). It is intriguing to speculate that acetylation of HMGA1b may modulate the protein's apoptotic potential, because acetylation of HMGA1b lysine 60 by P/CAF, similar to acetylation of HMGA1b lysine 54 by CBP on the β-IFN promoter, might affect its DNA-binding activity on other promoters or its association with other transcriptional factors involved in apoptosis. Moreover, we show that the HMGA1a isoform has a similar apoptotic effect, suggesting that it plays the same role as HMGA1b in cell cycle deregulation and apoptosis in normal rat thyroid cells.

We show that HMGA1 overexpression exerts an opposite effect on the growth of neoplastic *versus* normal cells: it is required for neoplastic transformation, whereas it induces G_2-M delay and apoptosis in normal cells. This suggests that the cell context plays an important role in determining whether HMGA overexpression causes cell proliferation or cell death. In the presence of such genetic alterations as active oncogene expression or inactivation of tumor suppressor genes, HMGA1b overexpression may protect neoplastic cells from apoptosis while exerting the opposite effect on normal cells. Similar results are reported for other genes, *e.g.*, *myc* (48). In serum-deprived cells, myc overexpression induces apoptosis, but

myc-expressing p53−/−, casp9−/−, and Apaf-1−/− cells were resistant to apoptosis after growth factor depletion (44).

Apoptosis is thought to be a default pathway in cells receiving conflicting cell proliferation signals (9, 48). Within this framework, we speculate that the proliferative input of HMGA1b overexpression, which allows cells to enter S-phase rapidly, and growth inhibitory signals from normal cells, which prevent completion of the G_2-M phase, can cause apoptosis.

ACKNOWLEDGMENTS

We thank Jean Ann Gilder for editing the text and Fernando Sferratore and Rosa Visone for excellent technical assistance. We also thank Enrico Avvedimento for helpful discussions about the cell cycle-related experiments.

REFERENCES

1. Johnson, K. R., Lehn, D. A., and Reeves, R. Alternative processing of mRNA's coding for human HMG I and HMG Y proteins. Mol. Cell. Biol., *9:* 2114–2123, 1989.
2. Manfioletti, G., Giancotti, V., Bandiera, A., Buratti, E., Sautiewre, P., Cary, P., Crane-Robinson, C., Coles, B., and Goodwin, G. H. cDNA cloning of the HMGI-c phosphoprotein, a nuclear protein associated with neoplastic and undifferentiated phenotypes. Nucleic Acids Res., *19:* 6793–6797, 1991.
3. Ferranti, P., Malori, A., Marino, G., Pucci, P., Goodwin, G. H., Manfioletti, G., and Giancotti, V. Mass spectrometric analysis of the HMGY protein from Lewis lung carcinoma. Identification of phosphorylation sites. J. Biol. Chem., *267:* 22486–22489, 1992.
4. Du, W., and Maniatis, T. The high mobility group protein HMG I (Y) can stimulate or inhibit DNA binding of distinct transcription factor ATF-2 isoforms. Proc. Natl. Acad. Sci. USA, *91:* 11318–11322, 1994.
5. Falvo, J. V., Thanos, D., and Maniatis, T. Reversal of intrinsic DNA bends in the *IFN β* gene enhancer by transcription factors and the architectural protein HMG I(Y). Cell, *83:* 1101–1111, 1995.
6. Grosschedl, R., Giese, K., and Pagel, J. HMG domain proteins: architectural elements in the assembly of nucleoprotein structures. Trends Genet., *10:* 94–100, 1994.
7. Thanos, D., and Maniatis, T. The high mobility group protein HMG I(Y) is required for NF-kB-dependent virus induction of the human *IFN-β* gene. Cell, *71:* 777–789, 1992.
8. Thanos, D., and Maniatis, T. Virus induction of human *IFN β* gene expression requires the assembly of an enhanceosome. Cell, *83:* 1091–1100, 1995.
9. Zhao, X., Gschwend, J. E., Thomas Powell, C., Foster, R. G., Day, K. C., and Day, M. L. Retinoblastoma protein-dependent growth signal conflict and caspase activity are required for protein kinase C-signaled apoptosis of prostate epithelial cells. J. Biol. Chem., *272:* 22751–22757, 1997.
10. Zhou, X., Benson, K. F., Ashar, H. R., and Chada. K. Mutation responsible for the mouse pygmy phenotype in the developmentally regulated factor HMGI-C. Nature (Lond.), *376:* 771–774, 1995.
11. Meijer, L., Ostvold, A. C., Walass, S. I., Lund, T., and Laland, S. G. High-mobility-group proteins P1, I, and Y as substrates of the M-phase-specific p34cdc2/cyclincdc13 kinase. Eur. J. Biochem., *196:* 557–567, 1991.
12. Nissen, M. S., Langan, T. A., and Reeves, R. Phosphorylation by cdc2 kinase modulates DNA binding activity of high mobility group I nonhistone chromatin protein. J. Biol. Chem., *266:* 19945–19952, 1991.
13. Reeves, R., Langan, T. A., and Nissen, M. S. Phosphorylation of the DNA-binding domain of nonhistone high-mobility group I protein by cdc2 kinase: reduction of binding affinity. Proc. Natl. Acad. Sci. USA, *88:* 1671–1675, 1991.
14. Chiappetta, G., Avantaggiato, V., Visconti, R., Fedele, M., Battista, S., Trapasso, F., Merciai, B. M., Fidanza, V., Giancotti, V., Santoro, M., Simeone, A., and Fusco, A. High level expression of the *HMGI (Y)* gene during embryonic development. Oncogene, *13:* 2439–2446, 1996.
15. Giancotti, V., Berlingieri, M. T., Di Fiore, P. P., Fusco, A., Vecchio, G., and Crane-Robinson, C. Changes in nuclear proteins following transformation of rat thyroid epithelial cells by a murine sarcoma retrovirus. Cancer Res., *45:* 6051–6057, 1985.
16. Giancotti, V., Pani, B., D'Andrea, P., Berlingieri, M. T., Di Fiore, P. P., Fusco, A., Vecchio, G., Philip, R., Crane-Robinson, C., Nicolas, R. H., Wright, C. A., and Goodwin, G. H., Elevated levels of a specific class of nuclear phosphoproteins in cells transformed with *ras* and v-*mos* oncogenes and by co-transfection with c-*myc* and polyoma middle T genes. EMBO J., *6:* 1981–1987, 1987.
17. Giancotti, V., Buratti, E., Perissin, L., Zorzet, S., Balmain, A., Portella, G., Fusco, A., and Goodwin. G. H. Analysis of the HMGI nuclear proteins in mouse neoplastic cells induced by different procedures. Exp. Cell Res., *184:* 538–545, 1989.
18. Berlingieri, M. T., Manfioletti, G., Santoro, M., Bandiera, A., Visconti, R., Giancotti, V., and Fusco, A. Inhibition of HMGI-C protein synthesis suppresses retrovirally induced neoplastic transformation of rat thyroid cells. Mol. Cell. Biol., *15:* 1545–1553, 1995.
19. Abe, N., Watanabe, T., Sugiyama, M., Uchimura, H., Chiappetta, G., Fusco, A., and Atomi, Y. Determination of high mobility group I(Y) expression level in colorectal neoplasias: a potential diagnostic marker. Cancer Res., *59:* 1169–1174, 1999.
20. Bandiera, A., Bonifacio, D., Manfioletti, G., Mantovani, F., Rustighi, A., Zanconati, F., Fusco, A., Di Bonito, L., and Giancotti, V. Expression of HMGI(Y) proteins in squamous intraepithelial and invasive lesions of the uterine cervix. Cancer Res., *58:* 426–431, 1998.
21. Fedele, M., Bandiera, A., Chiappetta, G., Battista, S., Viglietto, G., Manfioletti, G., Casamassimi, A., Santoro, M., Giancotti, V., and Fusco, A. Human colorectal carcinomas express high levels of high mobility group HMGI (Y) proteins. Cancer Res., *56:* 1896–1901, 1996.
22. Scala, S., Portella, G., Fedele, M., Chiappetta, G., and Fusco, A. Adenovirus-mediated suppression of HMGI(Y) protein synthesis as potential therapy of human malignant neoplasias. Proc. Natl. Acad. Sci. USA, *97:* 4256–4261, 2000.
23. Kazmierczak, B., Bol, S., Wanschura, S., Bartnitzke, S., and Bullerdiek, J. PAC clone containing the *HMGI(Y)* gene spans the breakpoint of a 6p21 translocation in a uterine leiomyoma cell line. Genes Chromosomes Cancer, *17:* 191–193, 1996.
24. Tkachenko, A., Ashar, H. R., Meloni, A. M., Sandberg, A. A., and Chada. K. K. Misexpression of disrupted HMGI architectural factors activates alternative pathways of tumorigenesis. Cancer Res., *57:* 2276–2280, 1997.
25. Xiao, S., Lux, M. L., Reeves, R., Hudson, T. J., and Fletcher, J. A. HMGI(Y) activation by chromosome 6p21 rearrangements in multilineage mesenchymal cells from pulmonary hamartoma. Am. J. Pathol., *150:* 901–910, 1997.
26. Williams, A. J., Powell, W. L., Collins, T., and Morton, C. C. HMGI(Y) expression in human uterine leiomyomata. Involvement of another high-mobility group architectural factor in a benign neoplasm. Am. J. Pathol., *150:* 911–918, 1997.
27. Dal Cin, P., Fusco, A., Belge, G., Chiappetta, G., Fedele, M., Pauwels, P., Bullerdiek, J., and Van den Berghe, H. Involvement of the *HMGI(Y)* gene in a microfollicular adenoma of the thyroid. Genes Chromosomes Cancer, *24:* 286–289, 1999.
28. Fusco, A., Portella, G., Di Fiore, P. P., Berlingieri, M. T., Di Lauro, R., Schneider, A. B., and Vecchio, G. A *mos* oncogene-containing retrovirus, myeloproliferative sarcoma virus, transforms rat thyroid epithelial cells and irreversibly blocks their differentiation pattern. J. Virol., *56:* 284–292, 1985.
29. Munshi, N., Merika, M., Yie, J., Senger, K., Chen, G., and Thanos, D. Acetylation of HMG I(Y) by CBP turns off IFN *β* expression by disrupting the enhanceosome. Mol. Cell, *4:* 457–467, 1998.
30. Graham, F. L., and van der Eb, A. J. A new technique for the assay of the infectivity of human adenovirus 5 DNA. Virology, *52:* 456–467, 1973.
31. Sambrook, J., Fritsch, E. F., and Maniatis, T. (eds.). Molecular Cloning: A Laboratory Manual, Ed. 2, chapter 7. Cold Spring Harbor, NY: Cold Spring Harbor Laboratory, 1989.
32. Chiappetta, G., Bandiera, A., Berlingieri, M. T., Visconti, R., Manfioletti, G., Battista, S., Martinez-Tello, F. J., Santoro, M., Giancotti, V., and Fusco, A. The expression of the high mobility group HMGI (Y) proteins correlates with the malignant phenotype of human thyroid neoplasms. Oncogene, *10:* 1307–1314, 1995.
33. Krishan, A. Rapid flow cytofluorometric analysis of mammalian cell cycle by propidium iodide staining. J. Cell Biol., *66:* 188–193, 1975.
34. Reed, S. I., Bailly, E., Dulic, V., Hengst, L., Resnitzky, D., and Slingerland, J. G_1 control in mammalian cells. J. Cell Sci., *18* (Suppl.)*:* 69–73, 1994.
35. Koff, A., Giordano, A., Desai, D., Yamashita, K., Harper, J. W., Elledge, S., Nishimoto, T., Morgan, D. O., Franza, B. R., and Roberts, J. M. Formation and activation of a cyclin E-cdk2 complex during the G_1 phase of the human cell cycle. Science (Wash. DC), *257:* 1689–1694, 1992.
36. Matsushime, H., Quelle, D. E., Shurtleff, S. A., Shibuya, M., Sherr, C. J., and Kato, J. Y. D-type cyclin-dependent kinase activity in mammalian cells. Mol. Cell. Biol., *3:* 2066–2076, 1994.
37. Sherr, C. J., and Roberts, J. M. Inhibitors of mammalian G_1 cyclin-dependent kinases. Genes Dev., *10:* 1149–1163, 1995.
38. Fernandes-Alnemri, T., Litwack, G., and Alnemri, E. S. CPP32, a novel human apoptotic protein with homology to *Caenorhabditis elegans* cell death protein Ced-3 and mammalian interleukin-1 *β*-converting enzyme. J. Biol. Chem., *269:* 30761–30764, 1994.
39. Nicholson, D. W., Ali, A., Thornberry, N. A., Vaillancourt, J. P., Ding, C. K., Gallant, M., Gareau, Y., Griffin, P. R., Labelle, M., Lazebnik, Y. A., *et al.* Identification and inhibition of the ICE/CED-3 protease necessary for mammalian apoptosis. Nature (Lond.), *376:* 37–43, 1995.
40. Schlegel, J., Peters, I., Orrenius, S., Miller, D. K., Thornberry, N. A., Yamin, T. T., and Nicholson. D. W. CPP32/apopain is a key interleukin 1 *β* converting enzyme-like protease involved in Fas-mediated apoptosis. J. Biol. Chem., *271:* 1841–1844, 1996.
41. Tewari, M., Quan, L. T., O'Rourke, K., Desnoyers, S., Zeng, Z., Beidler, D. R., Poirier, G. G., Salvesen, G. S., and Dixit, V. M. Yama/CPP32 *β*, a mammalian homologue of CED-3, is a poly(ADP-ribose) polymerase. Cell, *81:* 801–809, 1995.
42. Duriez, P. J., Desnoyers, S., Hoflack, J. C., Shah, G. M., Morelle, B., Bourassa, S., Poirier, G. G., and Talbot. B. Characterization of antipeptide antibodies directed towards the automodification domain and apoptotic fragment of poly (ADP-ribose) polymerase. Biochim. Biophys. Acta, *1334:* 65–72, 1997.
43. Polverino, A. J., and Patterson, S. D. Selective activation of caspases during apoptotic induction in HL-60 cells. Effects of a tetrapeptide inhibitor. J. Biol. Chem., *272:* 7013–7021, 1997.
44. Soengas, M. S., Alarcon, R. M., Yoshida, H., Giaccia, A. J., Hakem, R., Mak, T. W., and Lowe, S. W. Apaf-1 and caspase-9 in p53-dependent apoptosis and tumor inhibition. Science (Wash. DC), *284:* 156–159, 1999.
45. Yie, J., Liang, S., Merika, M., and Thanos, D. Intra- and intermolecular cooperative binding of high-mobility-group protein I(Y) to the *β*-interferon promoter. Mol. Cell. Biol., *17:* 3649–3662, 1997.
46. Chiappetta, G., Tallini, G., De Biasio, M. C., Manfioletti, G., Martinez-Tello, F. J., Pentimalli, F., de Nigris, F., Mastro, A., Botti, G., Fedele, M., Berger, N., Santoro, M., Giancotti, V., and Fusco, A. Detection of high mobility group I HMGI(Y) protein in the diagnosis of thyroid tumors: HMGI(Y) expression represents a potential diagnostic indicator of carcinoma. Cancer Res., *58:* 4193–4198, 1998.
47. Tamimi, Y., van der Poel, H. G., Denyn, M. M., Umbas, R., Karthaus, H. F. M., Debruyne, F. M., and Shalken, J. A. Increased expression of high mobility group protein I (Y) in high grade prostate cancer determined by *in situ* hybridization. Cancer Res., *53:* 5512–5516, 1993.
48. Evan, G. I., Brown, L., Whyte, M., and Harrington, E. Apoptosis and the cell cycle. Curr. Opin. Cell Biol., *7:* 825–834, 1995.